Tellus (2000), 52A, 554–565
Printed in UK. All rights reserved

TELLUS
ISSN 0280–6495

Southern Ocean transformation in a coupled model with and without eddy mass fluxes

By KEVIN SPEER[1]*, ERIC GUILYARDI[2] and GURVAN MADEC[2], [1]*LPO/IFREMER/CNRS, B.P. 70, 29280, Plouzane, France;* [2]*LODYC, Univ. Paris VI, 4 pl. Jussieu, 75000, Paris, France*

(Manuscript received 23 February 1999; in final form 22 February 2000)

ABSTRACT

A coupled air–sea general circulation model is used to simulate the global circulation. Different parameterizations of lateral mixing in the ocean by eddies, horizontal, isopycnal, and isopycnal plus eddy advective flux, are compared from the perspective of water mass transformation in the Southern Ocean. The different mixing physics imply different buoyancy equilibria in the surface mixed layer, different transformations, and therefore a variety of meridional overturning streamfunctions. The coupled-model approach avoids strong artificial water mass transformation associated with relaxation to prescribed mixed layer conditions. Instead, transformation results from the more physical non-local, nonlinear interdependence of sea-surface temperature, air–sea fluxes, and circulation in the model's atmosphere and ocean. The development of a stronger mid-depth circulation cell and associated upwelling when eddy fluxes are present, is examined. The strength of overturning is diagnosed in density coordinates using the transformation framework.

1. Introduction

Coarse resolution circulation models needed for climate simulations are obliged to parameterize the effects of unresolved motion, and often do so with a downgradient diffusive flux of properties. Advective effects of unresolved flow may be as important as diffusive effects, and recent efforts to include advection in coarse ocean models focus on eddy-induced velocities proportional to lateral layer thickness gradients (Danabasoglu and McWilliams, 1995; Hu, 1997; Hirst and McDougall 1998). These effects are particularly striking in the above simulations for the modifications they make to the meridional circulation in the Southern Ocean, because of the great distance over which the relatively small ageostrophic flows can accumulate. The southward deep flow and northward surface flow that dominates the discussion of meridional circulation, or Deacon Cell, is found to decrease with the increasing strength of the (parameterized) eddy velocities. This issue has been revisited and reviewed in Marsh et al. (2000) specifically to address Southern Ocean meridional circulation, as well as the relation between this circulation and interior and surface layer fluxes, in a coarse resolution ocean model.

The relation between the Deacon Cell and surface fluxes is the crux of the matter. Although previous coarse resolution model studies have emphasized the Deacon Cell's dependence on eddy advection, they have overlooked the nature of buoyancy gain and loss in the Southern Ocean, and the implications for particular water masses. The issue of compatibility between surface buoyancy flux and near-surface ageostrophic flow has been clearly discussed by Tandon and Garrett

* Corresponding author address: Florida State University, Department of Oceanography, Tallahassee, FL. 32306 USA.
e-mail: kspeer@ocean.fsu.edu

(1996) and by Marshall (1997), in the framework of water mass transformation (Walin, 1982; Garrett et al., 1995; Speer, 1997). Marshall's (1997) idealised Deacon Cells, one with zero surface buoyancy flux and one with surface buoyancy loss, illustrate the adjustment of the oceanic density field to produce eddy fluxes compatible with surface transformation. In both cases, the Eulerian mean circulation is the same, with southward geostrophic flow below a topographic sill; however, in the first case transport is zero since the eddy-induced flow cancels Eulerian velocity completely, while in the second case with buoyancy fluxes a net circulation remains, with an overturning cell in equilibrium with the fluxes. In general, the surface buoyancy flux depends on the circulation (oceanic and atmospheric), and local, linearized prescriptions a priori of this flux in models are problematic. We show that neither of two limits examined by Marshall (1997) represent the solutions of the coupled model, which, for overall thermodynamic balance, shows a region of buoyancy gain at Southern Ocean latitudes.

To the degree that resolution permits, coupled models represent the complicated interdependence of fluxes and sea-surface temperature; hence, we avoid some inconsistencies by using a coupled ocean-atmosphere model to generate the Deacon Cell, and go further to consider different eddy parameterizations (Guilyardi 1998). The question of realism is still pertinent, and we can compare our results to observations (COADS) that have been found by inverse methods to be consistent with Southern Ocean circulation (Sloyan, 1997; Sloyan and Rintoul, 2000). Our goal is to show how the transformation derived from surface fluxes is related to the (diapycnal) meridional circulation in our coupled model, and that the upwelling branch of the Deacon Cell switches from a deep southward geostrophic flow without eddy advection to a less deep southward eddy-driven flow when eddies are included. For the water masses as they are represented in the model, this implies a greater component of low oxygen Upper Circumpolar Deep Water in the upwelling branch of the Deacon Cell.

Note that our definition of the Deacon Cell is fundamentally diabatic: the amplitude of the intermediate overturning streamfunction in latitude-density coordinates. In our runs this cell is centered near 50°S and a density of 27 ($g\,cm^{-3}$; density anomaly units are assumed throughout).

Ocean simulations in both forced and coupled modes were carried out. In forced mode, SST and heat flux remain close to climatology regardless of the mixing parameterization, while sensitivity to mixing parameterizations is much greater in the coupled mode. This lack of sensitivity of either heat flux or SST in forced mode made comparisons between coupled simulations and forced simulations fruitless, so forced mode solutions are not described here. The emphasis is rather on a developing a framework for diagnosing the diabatic response of the coupled model simulations, especially to investigate the meridional overturning cell and associated cross-isopycnal fluxes.

2. The model and numerical experiments

The model has been fully described by Guilyardi and Madec (1997), so we only summarize the essential elements below (Subsections 2.1–2.3). Subsection 2.4 describes the application of different mixing parameterizations.

2.1. The OPA model

The OPA8 ocean GCM has been developed at the Laboratoire d'Océanographie DYnamique et de Climatologie (LODYC) (Madec et al., 1998). It solves the primitive equations with a non-linear equation of state. A rigid lid is assumed at the sea surface. The code has been adapted to the global ocean by Madec and Imbard (1996). Horizontal space resolution is roughly equivalent to a geographical mesh of 2 by 1.5° (with a meridional resolution of 0.5° near the equator), and vertical resolution is 31 vertical levels, with 10 levels in the top 100 m. The model time step is 1 h 40′. Vertical eddy diffusivity and viscosity coefficients are computed from a 1.5 turbulent closure scheme (Blanke and Delecluse 1993) which allows an explicit formulation of the mixed layer as well as minimum diffusion in the thermocline. Zero fluxes of heat and salt and no-slip conditions are applied at solid boundaries. Sea-ice is restored towards observations at high latitudes. Horizontal mixing of momentum is of Fickian type with an eddy viscosity coefficient of $4 \cdot 10^4\,m^2\,s^{-1}$, reduced in the Tropics to reach $2 \cdot 10^3\,m^2\,s^{-1}$ at the equator.

The lateral mixing of tracers (temperature and salinity) is described in Subsection 2.4.

There is no implementation of an ice model in the ocean, only restoring conditions to climatology. This constitutes an effective flux correction term wherever ice occurs in the climatology, and is the only such term in the model.

2.2. The ARPEGE model

The ARPEGE-climat (Version 2) atmosphere GCM, from CNRM/Météo-France, is a state of the art spectral atmosphere model developed from the ARPEGE/IFS weather forecast model (Déqué et al., 1994). The ARPEGE model used in this study is based on the version described by Guilyardi and Madec (1997) with the following differences. The model now has 19 vertical levels (with an increased resolution in the troposphere) and a triangular spectral T31 truncation is used for horizontal resolution corresponding to a 3.75° grid size. The convective entrainment rate is increased at lower levels, the radiation scheme is now based on the Fouquart-Morcrette scheme and a parameterisation of marine strato-cumulus is added.

2.3. Coupling procedure and initialization

The coupling procedure is similar to the one described in Guilyardi and Madec (1997): synchronous coupling with a daily exchange of fluxes. Version 2.0 of OASIS is used (Terray et al., 1996) in which the SST of a given AGCM grid-square is now the weighted average of the underlying OGCM sea grid points. The river runoffs are computed using 81 river drainage basins defined on the AGCM grid and are passed instantaneously to corresponding river mouth ocean grid points. The initial state of the ocean is based on the atlas of Levitus (1982) followed by a short dynamic spin-up (Madec and Imbard 1996, Guilyardi and Madec 1997), and no artificial flux corrections are applied at the air–sea interface (except in sea-ice regions).

2.4. The 3 sensitivity experiments

Based on the coupled model described above, a sensitivity study to ocean lateral diffusion of tracer is made. The reference experiment (cm1) is integrated for 40 years. It uses a classical horizontal harmonic diffusion scheme, with an eddy diffusivity coefficient K_H of $2000\,m^2\,s^{-1}$. As noted by many authors, this horizontal diffusion scheme generates spurious diapycnal fluxes where the isopycnals are steeply sloping. In OPA, a strategy has been chosen to overcome this problem: a local horizontal filtering of the isopycnals slope is made prior to the computation of the isopycnal diffusion operator (Guilyardi and Madec, 1997). This prevents the development of grid-point noise so that no artificial background horizontal mixing has to be added (thus allowing "pure" isopycnal mixing). A 40-year coupled simulation is performed using the OPA pure isopycnal diffusion scheme (experiment cm2) with an eddy diffusivity coefficient K_I of $2000\,m^2\,s^{-1}$.

Baroclinic instability is a significant source of mixing within the ocean. In order to mimic this process, Gent and McWilliams (1990, GM90 thereafter) proposed a quasi-adiabatic parameterisation in which an eddy-induced advection is added to the tracer equation (Gent et al., 1995). The eddy-induced velocity proposed by GM90 is proportional to the gradient of the slope of the isopycnal ($U^* = K_{eiv}\nabla\cdot[\text{slope}]$) and therefore tends to flatten density fronts. The third 40-year simulation (experiment cm3) includes such an eddy-induced advection, in addition to the isopycnal diffusion, with $K_{eiv} = K_I = 2000\,m^2\,s^{-1}$. This value of K_{eiv} is quite high for most ocean regions when compared to those estimated in the literature (Visbeck et al., 1997). It is nevertheless kept at $2000\,m^2\,s^{-1}$ to magnify its effect in the model. The surface boundary condition of U^* was not discussed by GM90 and is not straightforward to choose (Tréguier et al., 1997; Marshall, 1997). In this first implementation of GM90 in OPA, the slopes are bounded by 1/100 everywhere, this limit linearly decreasing to zero between 70 m depth and the surface.

Surface air–sea fluxes in the simulations are shown in Fig. 1. Compared to the COADS climatology, the most important differences are that in the model Southern Ocean, the maximum zonal wind stress is nearly a factor of two greater, and the fresh water flux is reduced. The model also tends to gain overall more heat than is observed, apparently the result of a deficiency in the atmospheric boundary layer representation of clouds (Guilyardi and Madec, 1997). The response of the

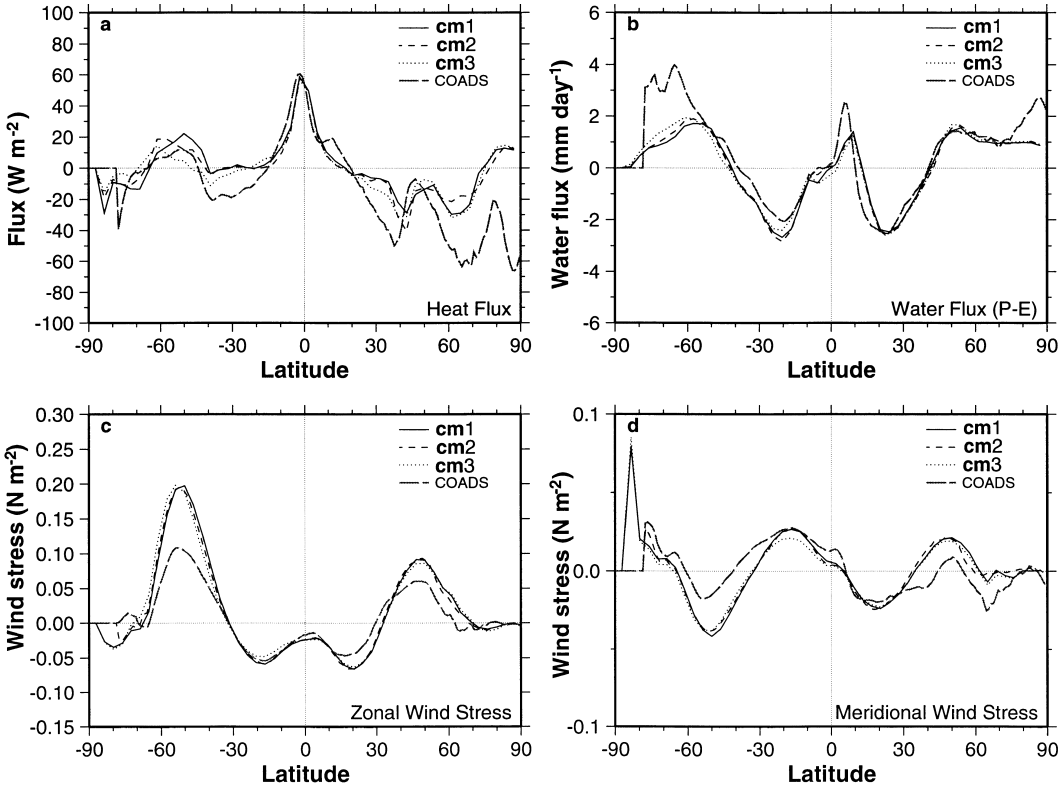

Fig. 1. Zonal mean of air–sea fluxes. Average of years 26–40 for simulations; COADS climatology by Da Silva et al. (1994). (a) downward heat flux, (b) fresh water flux ($P-E$), (c) zonal wind stress and (d) meridional wind stress.

model in the three configurations is described in Guilyardi (1998). In the runs with isopycnal mixing rather than horizontal mixing, he noted an additional warming after 40 years of up to 3°C in places in the Southern Ocean. This heating was the result of an excess air–sea heat flux being confined to the mixed layer by isopycnal mixing (whereas with horizontal mixing the heat was redistributed in the interior of the ocean).

Here, we are concerned with the conversion of water from one density class to another and with the the meridional circulation in the Southern Ocean part of the model. None of the thermodynamic details of the coupled simulations carried the model far away from its initial state after 40 years. Longer integrations will very likely reveal water mass evolution owing to incompatibilities between fluxes and stratification, that is, model fluxes will not support the water mass structure over the long term. However, model drift was weak (see below), even without flux correction (except for sea-ice), and is ignored here; the compatibility is shown quantitatively by diagnosing the transformation.

3. Transformation and advection

The air–sea forcing is written in terms of a transformation from one density (ρ, or σ for density anomaly) or buoyancy ($b=-g\rho/\rho_0$) class to another:

$$F(b)=\int_{\text{year}} \mathrm{d}t \iint_{\text{area}} -B\,\mathrm{d}x\,\mathrm{d}y\,\delta[b(x,y,t)-b'], \tag{1}$$

with the buoyancy flux

$$B=-\frac{g\alpha}{\rho_0 C_\mathrm{p}}\mathscr{H}(x,y,t)+\frac{g\rho(T,0)\beta S}{\rho_0(1-S)}\mathscr{W}(x,y,t), \tag{2}$$

where $\mathscr{H}(x, y, t)$ and $\mathscr{W}(x, y, t)$ are the surface fluxes of heat and fresh water (evaporation minus precipitation). Both are functions of location and time, assumed to vary periodically with the seasonal cycle. Given the temperature and salinity of the surface water $T(x, y, t)$ and $S(x, y, t)$, it is possible to calculate the buoyancy flux as function of the surface buoyancy. The delta function appearing in the integral is zero whenever the surface buoyancy b' is not equal to the buoyancy b, and therefore samples the surface flux only for surface water of buoyancy b. These quantities are calculated off-line at monthly intervals (the same result obtains using 5-day averages). Dividing by one year yields the annual average. For convenience, $F(b)$ or $F(\rho)$ is called the transformation by air–sea fluxes and its derivative with respect to buoyancy or density the formation.

Define the net advective volume flux across isopycnals A and the diffusive flux across isopycnals D by their integral along an isopycnal from a control surface to the sea surface:

$$A = \int_b (\boldsymbol{u} \cdot \boldsymbol{n})\, \mathrm{d}S, \tag{3}$$

where $\boldsymbol{n}$ is the unit normal vector to isopycnals, $\boldsymbol{u}$ is the velocity, and $\mathrm{d}S$ is the isopycnal surface area element, and

$$D = \int_b -\kappa \frac{\partial b}{\partial n}\, \mathrm{d}S, \tag{4}$$

where κ is the diapycnal diffusivity. The volume flux across isopycnals is usefully divided into the Ekman transport (A_{ek}), from the part of the integral over the Ekman layer, and a remainder, representing interior and other boundary fluxes. When diffusion is weak, motion is dominantly along isopycnals. In the extreme case of an ideal, adiabatic interior, for instance, both A and D are zero there and no cross-isopycnal motion occurs. In the Southern Ocean, where isopycnals strongly slope up toward the surface, water parcels may experience large vertical excursions along isopycnals, without mixing. Thus, upwelling can be the result of an upward adiabatic motion in the interior, and a final diabatic motion in the upper layers of the ocean where mixing is stronger and surface fluxes converge. The exact history of a water parcel's motion depends strongly on the mixing parameterization of the model. We focus here on methods to reveal the net, integrated cross-isopycnal transport in the model.

Mass and buoyancy conservation equations can be combined to form the water mass *transformation* equation:

$$F - A - \frac{\partial D}{\partial b} = 0, \tag{5}$$

(Walin, 1982), and the water mass *formation* equation:

$$\frac{\partial v}{\partial t} = -\frac{\partial \Psi^{\mathrm{e}}}{\partial b} - \frac{\partial F}{\partial b} + \frac{\partial^2 D}{\partial b^2}, \tag{6}$$

valid at all times. This equation relates layer volume v to the streamfunction at the control surface, surface air–sea forcing, and mixing or diffusion.

For easier comparison to earlier work, potential density is used as the primary variable in the following. For the interior streamfunction, potential density σ is adequate since we are interested essentially in the upper 2500 m of the water column.

Then, we have

$$\Psi^{\mathrm{e}}(\sigma) - F(\sigma) = \frac{\partial D}{\partial \sigma}, \tag{7}$$

where F is now defined to be positive for buoyancy loss or density gain. The control surface may be chosen for convenience, for instance as the base of the winter mixed layer.

The initial state of the three simulations is obtained as follows. From Levitus (1982) hydrography and from a state at rest, a 10-year dynamic spin-up is performed where the ocean-only component is forced by monthly-varying climatological wind stress (Hellerman and Rosenstein, 1983), and by heat and fresh water fluxes (Esbensen and Kushnir, 1981; Oberhuber, 1988) in robust-diagnostic mode (relaxation on temperature and salinity in the interior of the ocean, away from equator and all boundaries). From this ocean initial state, the fully coupled model is then integrated for 40 years in each case, with no flux corrections (except for sea-ice regions). Transformation, formation, and Ekman fluxes are computed from the resulting model monthly mean fields, using a density bin of $\delta\sigma = 0.2$.

In all 3 simulations, the zonal wind stress is greater than observations (Fig. 1) near 50°S. The difference may be partly due to undersampling in

the observational dataset, and the resulting underestimate of wind stress. However, the models have a number of parameterized atmospheric frictional processes which may not be correct, leading to an excess north-south temperature gradient and strong zonal winds. As a result, Ekman transports are also larger than observed, potentially driving a uniformly strong Deacon Cell. But as will be shown, the overturning or cross-isopycnal meridional cell strength revealed by the transformation analysis shows a dependence on mixing physics and buoyancy fluxes.

The fluxes from the three simulations after 40 years show transformation rates that have evolved from initial values to a state that is in better overall agreement with the newer COADS climatology, especially at intermediate densities (Fig. 2a). At higher density classes, the differences are significant, but the form is similar (Fig. 2b), with buoyancy gain at higher density and buoyancy loss at lower density. Thus, parcels at the surface can move north in Ekman flow and gain buoyancy (and temperature) as they move, while parcels at lower density on the northern side of the Circumpolar Current lose buoyancy and form deep mixed layers. The Ekman drift, forced by wind stress, is the primary dynamical mechanism bringing colder water north to experience warmer atmospheric temperatures and gain heat. (Meanders of the Circumpolar Current are another mechanism for bringing cold water north). This structure, with buoyancy gain to the south ($\sigma > 26$–26.5) and buoyancy loss to the north ($\sigma < 26$–26.5) is of fundamental importance for cross-isopycnal motion in the Deacon Cell, allowing a net mass exchange between dense layers and the thermocline. The coupled model preserves this structure, implying (for weak diffusion) that water upwells, gains buoyancy and flows north to lower density classes in the Ekman layer, then converges, forming water masses in lower density classes, or mode water density classes.

Doney et al. (1998) find a similar structure in their coupled model simulation, but they focus on the occurence of heat loss over mode waters and very dense antarctic coastal waters. Our coupled model needs an improved physical representation of sea-ice formation and the spreading of dense water in boundary plumes to be confident of results for these water masses. The dense formation close to the continent is not well enough resolved here in either the data or the model to be of use, so we do not discuss circulation and transformation in the maximum density classes of coastal and bottom water.

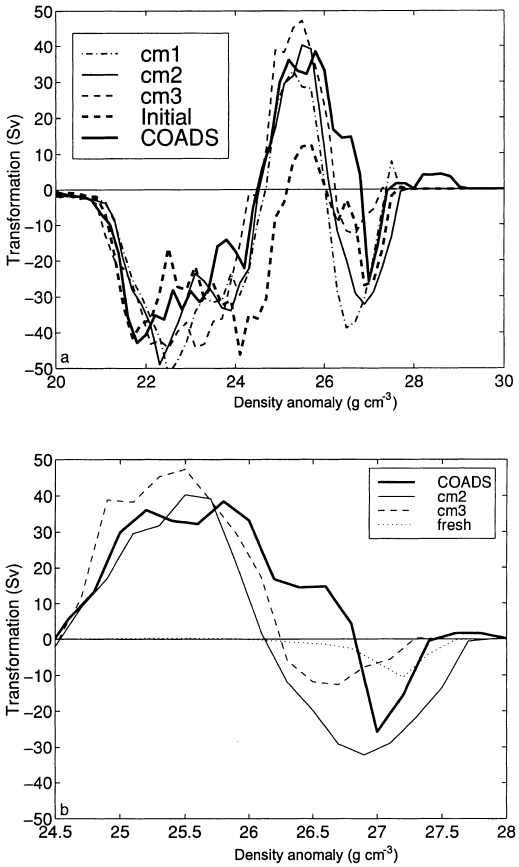

Fig. 2. (a) Transformation in the Southern Hemisphere of the three coupled model simulations years 39–40), the common model initial state, and COADS (from heat flux only; positive values are buoyancy loss). (b) Close up of high density range, with an estimate of the fresh water flux contribution to transformation based on an adjusted COADS fresh water flux. The adjustment is essentially a reduction by 1–2 mm day^{-1} at high latitudes.

The buoyancy gain noted above occurs at quite different density classes in cm2 and cm3 (Fig. 2b), with the gain at lower density in cm3 than in cm2, and the formation spread over a much greater density range in cm2 than in cm3. Both model runs show formation at lower density (25.5–26.5) than the COADS data (26–27), hence they tend to form mixed layers (mode water) at lower density

(or higher temperatures) than the ocean. The COADS curve is derived from heat flux alone; adding an estimate of the fresh water component (Fig. 2b) would not modify these conclusions. The strong transformation in the case of cm2 is a result of strong winds, together with weak mixing and eddy fluxes; either of these processes tends to reduce transformation by mixing water across isopycnals in the surface layers, and thereby cancelling some of the effect of the surface fluxes. Thus, the weakness of the cm3 transformation is connected to the presence of eddy velocities partially cancelling surface Ekman layer flow. This aspect is discussed next.

4. Net meridional circulation

The net meridional circulation streamfunction is calculated from velocity averaged on potential density surfaces over the last two years of each 40-year run (Figs. 3, 4; only results south of 30°S are presented). The runs are close to a periodic, seasonal cycle and the time average represents a net advection across isopycnals. Also displayed are the transformation F and Ekman transport A_{Ek}. Overall, there is a southward flow of water near the surface at low densities and equatorward of 30°S (not shown), and a northward near-surface flow at higher latitudes. A small circulation cell at very high densities is due to the export of bottom water. (In these very high density classes, some bottom water flow is mixed together with the deep water flow because of the coarse resolution in density classes and because of the potential density variable itself, which does not exactly separate isopycnal and diapycnal processes at depth. These distinctions are not crucial here.)

In the isopycnal run, both F and streamfunction increase to about 20×10^6 m^3 s^{-1} near 27.6, but F continues to increase to 30×10^6 m^3 s^{-1} at 26.9, while streamfunction attains about 25×10^6 m^3 s^{-1}. The increase is matched by increasing Ekman transport to lower density, illustrating the upwelling and northward transport of the Deacon Cell. Note that the upwelling into the mixed layer is confined principally to densities greater than 27.6, which (in this simulation) lie mainly below topographic features, so that the southward flow feeding this upwelling is simply geostrophic flow in boundary currents.

Water leaves the mixed layer and re-enters the interior over the density range roughly corresponding to formation (25.5–26.5). Clearly the advective balance changes from a simple Ekman transport over these lower densities, probably because of interaction with several oceanic gyres, but the exact mechanism is not identified without

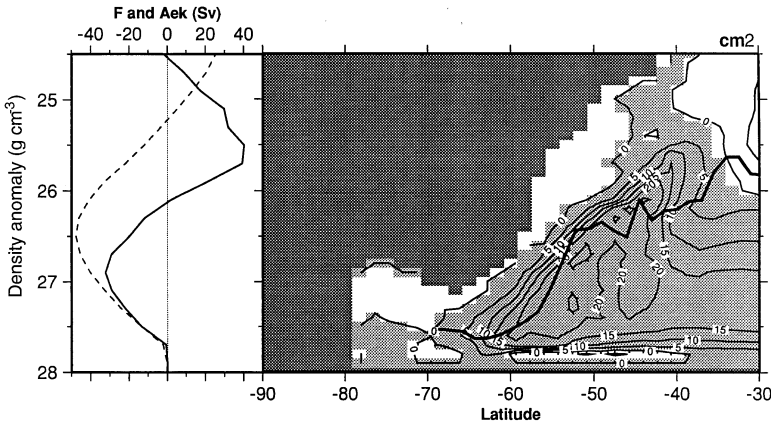

Fig. 3. Meridional streamfunction ($\times 10^6$ m^3 s^{-1}; gray is clockwise) in potential density versus latitude coordinates for the model Southern Ocean, run cm2 (year 40), together with the zonally averaged maximum mixed layer depth (heavy solid line). The streamfunction shows the overturning cell in which water denser than about 27 moves south and upwells into the surface mixed layer. A weak, deeper and denser cell in the opposite sense is also visible, as well as a tropical cell at densities less than about 26. Transformation and Ekman transport are displayed, with negative values corresponding to conversion to lower density and northward transport (left).

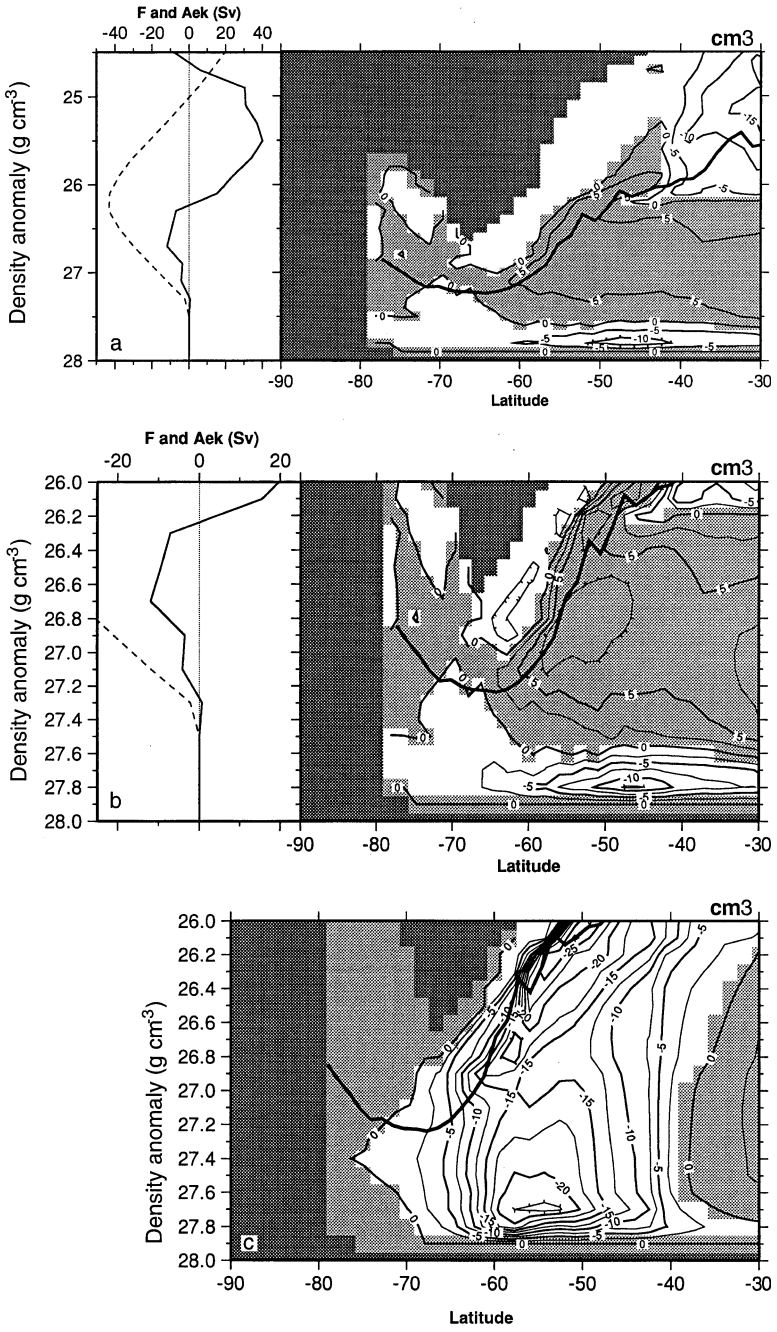

Fig. 4. (a) Meridional streamfunction ($\times 10^6$ m^3 s^{-1}; gray is clockwise) in potential density versus latitude coordinates for the model Southern Ocean, run cm3 (year 40), together with the zonally averaged maximum mixed layer depth (heavy solid line). Transformation and Ekman transport are displayed, with negative values corresponding to conversion to lower density and northward transport (left). (b) Close-up of run cm3, and (c) streamfunction for eddy advection term alone.

further decomposition of velocity and an examination of the detailed routes followed by water parcels.

In the simulation with eddy advection cm3, the overturning, associated upwelling, and F are much reduced (Figs. 4a, b). Moreover, the upwelling occurs at lower densities (27–27.6) than the previous case cm2, and no net upwelling appears at higher density. The meridional transport generated by the eddy advection term alone (Fig. 4b, lower), drives a southward transport of about 7×10^6 m^3 s^{-1} in the layers 27–27.6; superimposed on this circulation is a stronger boundary effect with southward transport near the surface and northward transport near the bottom. Hence, the strong transport in the Ekman layer carrying water north in the mixed layer has been greatly reduced by the eddy advection, leaving a relatively weak overturning cell. However, now the southward motion and upwelling is occuring over a broader, lower density range, corresponding to a shallower water mass. We can understand this effect by considering the stratification in the simulations and in the Levitus dataset.

The isopycnal layers with upwelling into the mixed layer are those with substantial north–south thickness gradients (Fig. 5). Levitus density shows the basic decreasing stratification at deeper levels (higher densities), relatively thick mode waters lighter than 27, and strong lateral thickness gradients from 27.2 to 27.6. This structure is well preserved in the isopycnal mixing run cm2, but the gradients are nearly eliminated in cm3. The strong thickness gradient layer spans the low oxygen layers in the Levitus climatology (Table 1), indicating that the upwelling water mass in cm3 is Upper Circumpolar Deep Water rather than the denser North Atlantic Deep Water.

Table 1. *Potential density of property extrema approximately indicating water mass cores, from the zonally averaged Levitus data at 42.5°S*

σ_θ	Property	Water mass
27.0		
27.2	salinity minimum	AAIW
27.4		
27.6	oxygen minimum	UCDW
27.8	salinity maximum	NADW
28.0		

Eddy fluxes are the only obvious mechanism available to flush upper circumpolar deep water southward, since this water mass lies mainly above the major topographic features and north-south ridges, and across a zonally unbounded latitude range. So the presence of eddy fluxes has shifted dramatically the structure of the overturning from a deep geostrophic southward flow of NADW toward a shallower UCDW contribution. In either case the Ekman transport returns water northward in the surface layers, but in the case with eddy fluxes much of the return is cancelled, and the overall strength of the cell is greatly reduced. Transformation is similarly reduced in this case, because eddy fluxes are captured by this quantity, illustrating the role of such fluxes in the buoyancy balance of the meridional circulation.

5. Discussion

The coupled model simulations consistently represent the air–sea feedbacks and interdependence of both water mass transformation and circulation. These coarse resolution simulations are designed to aid the identification of key processes in a thermodynamically consistent framework. The basic processes investigated here are those intimately connected to the meridional overturning in the Southern Ocean, the Ekman transport and the eddy-induced velocity, both ageostrophic flows that carry heat, mass and other properties across the zonally open latitudes of the Drake Passage. These flows are not independent from the thermodynamic balances in the model, and it is unphysical to separate a wind-driven overturning from a buoyancy driven one. The strength of the model is to show this dependence consistently, in terms of air–sea interactions, and explicitly, via an analysis of the modified transformation rates. Conversely, model weaknesses are revealed, especially an apparent exagerated eddy effect in the case of cm3. The model winds are too strong in the Southern Hemisphere, thus the exact relative equilibrium between various processes cannot be realistic; however, the basic arguement connecting circulation and air–sea fluxes is not affected by this flaw, and the fluxes themselves are qualitatively well represented, in particular the zone of heat or buoyancy gain at latitudes roughly 45–60°S (Fig. 1).

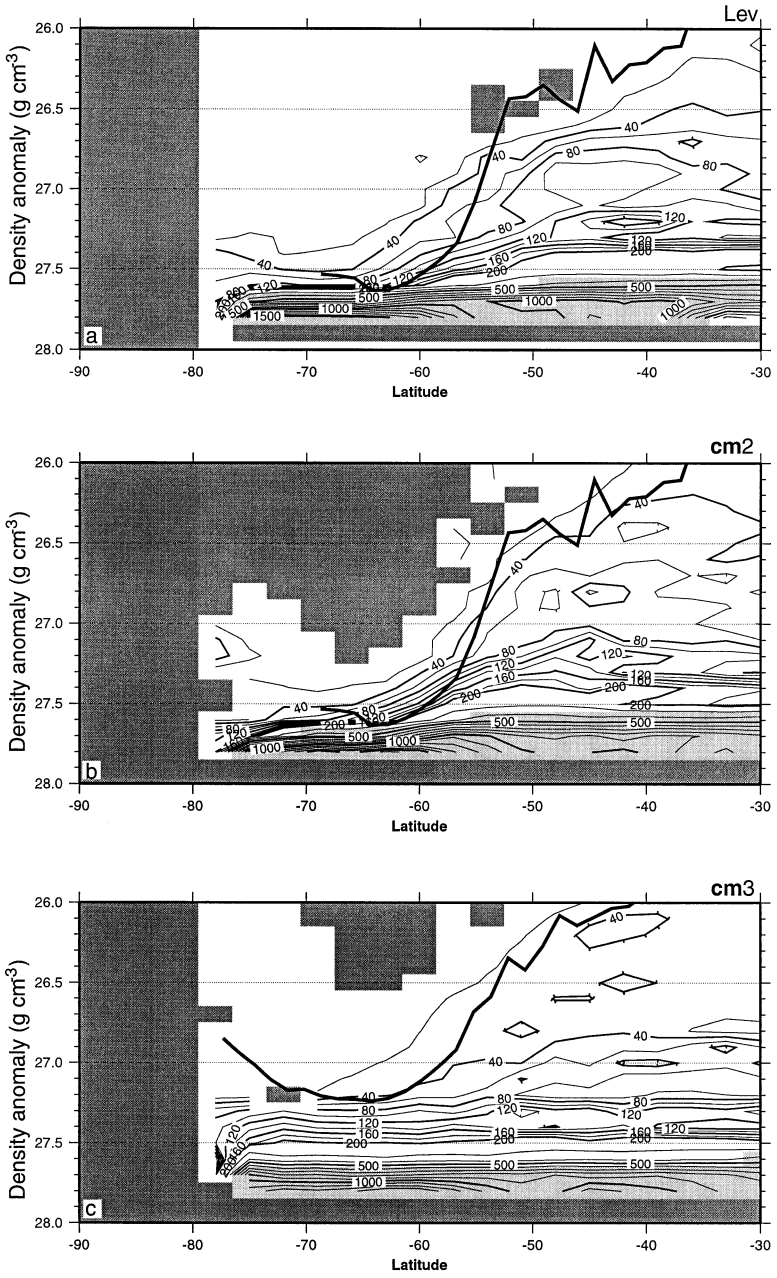

Fig. 5. Zonally averaged thickness between isopycnal layers separated by 0.1σ; Levitus (upper panel), year 40 of run cm2 (middle panel), and year 40 of run cm3 (lower panel). Zonally averaged maximum mixed layer depth is included (heavy solid line).

The eddy advection coefficient used here is strong ($2000\,m^2\,s^{-1}$) and constant. A smaller coefficient or one which varies in space or time will likely give different results, but the basic tendency to create a mass transport where there are thickness gradients will remain. Our goal is not to argue that the model does a better job of simulating the ocean when eddy fluxes are included — in certain respects the simulation with eddy fluxes is worse than the isopycnal mixing case without eddy fluxes. Our goal is rather to investigate the consequences of eddy fluxes in a coupled model via a plausible parameterization of their effects; the basic tendency to create a mass transport where there are thickness gradients modifies overturning and the basic heat and mass balances of the circulation. In this rather intense case of eddy advection, the circulation switches to a shallower upwelling mode, and the deep geostrophic flow is cancelled. The real situation may be somewhere in between, and perhaps an indication of just where is available in the transformation diagrams. From this information, the inclusion of eddy advection helps to move the transformation toward observed values; on the other hand, until the wind stress is more tightly constrained by observational analyses, little can be said about the degree of improvement.

We show here that stratification, eddy fluxes, and sea-surface buoyancy fluxes are strongly interrelated, and that their effects can be quantified and diagnosed within the density coordinate framework of transformation. Forced models may not well represent the solutions of the coupled model, which, for overall thermodynamic balance, require a region of buoyancy gain at Southern Ocean latitudes. This suggests that ocean circulation models with specified surface fluxes or relaxation fluxes may not be able to represent realistic transports, since they have to generate a stratification compatible with the (incorrect) fluxes. This stratification, in turn, is not likely to support acceptable eddy fluxes. So the degrees of freedom offered by the coupled model appear to be crucial to a diagnosis of overturning circulation in the Southern Ocean. An analysis of transformation provides the framework for comparing various approaches with each other and with observations.

The region of buoyancy gain or heat gain in the coupled model may be related to the geometry of the continents. SST is colder in the Southern Ocean than in the northern hemisphere oceans at similar latitudes because of the absence of continents, which in the northern hemisphere support boundary currents carrying warm water poleward. Atmospheric radiation is, on the other hand, rather symmetric in the mean, producing a tendency for the ocean to lose heat at high northern latitudes and to gain heat in the Southern Ocean.

6. Acknowledgments

This work was initiated while EG was at CERFACS, Toulouse, with the support of L. Terray. KGS and GM received support from the CNRS and the PATOM.

REFERENCES

Blanke, B. and Delecluse, P. 1993. Low-frequency variability of the tropical Atlantic Ocean simulated by a general circulation model with mixed-layer physics. *J. Phys. Oceanogr.* **23**, 1363–1388.

Danabasoglu, G. and McWilliams, J. C. 1995. Sensitivity of the global ocean circulation to parameterizations of mesoscale tracer transports. *J. Climate* **8**, 2967–2987.

da Silva, A. M., Young, C. C. and Levitus, S. 1994. Atlas of surface marine data 1994, vol. 3. *Anomalies of heat and momentum fluxes*. NOAA Atlas NESDIS 8, US Department of Commerce, NOAA, NESDIS.

Déqué, M., Dreveton, C., Braun, C. and Cariolle, D. 1994. The climate version of Arpege/IFS: a contribution to the French community climate modeling. *Climate Dyn.* **10**, 249–266.

Doney, S. C., Large, W. G. and Bryan, F. O. 1998. Surface ocean fluxes and water-mass transformation rates in the coupled NCAR Climate System Model. *J. Climate* **11**, 1422–1443.

Esbensen, S. K. and Kushnir, V. 1981. *The heat budget of the Global Ocean: an atlas based on estimates from marine surface observations*. Climatic Research Institution 29, Oregon Sate University, Corvallis, USA.

Garrett, C., Speer, K. G. and Tragou, E. 1995. The relationship between water mass formation and the surface buoyancy flux, with application to Phillips' Red Sea model. *J. Phys. Ocean* **25**, 1696–1705.

Gent, P. R. and McWilliams, J. C. 1990. Isopycnal mixing in ocean circulation models *J. Phys. Oceanogr.* **20**, 150–155.

Gent, P. R., Willebrand, J., McDougall, T. and McWilli-

ams, J. C. 1995. Parameterizing eddy-induced tracer transports in ocean circulation models. *J. Phys. Ocean* **25**, 463–474.

Guilyardi, E. and Madec, G. 1997. Performance of the OPA/ARPEGE-T21 global ocean–atmosphere coupled model. *Climate Dyn.* **13**, 149–165.

Guilyardi, E. 1997. *Rôle de la physique océanique sur la formation/consommation des masses d'eau dans un modèle couplé océan–atmosphepe*. Université Paul Sabatier, Toulouse, France, 197 pp.

Hellerman, S. anad Rosenstein, M. 1983. Normal monthly wind stress over the world ocean with error estimates. *J. Phys. Oceanogr.* **13**, 1093–1104.

Hirst, A. C. and McDougall, T. J. 1998. Meridional overturning and dianeutral transport in a z-coordinate ocean model including eddy-induced advection. *J. Phys. Oceanogr.* **28**, 1205–1223.

Hu, D. 1997. Global-scale water masses, meridional circulation, and heat transport simulated with a global isopycnal ocean model. *J. Phys. Oceanogr.* **27**, 96–120.

Ledwell, J. R., Watson, A. J. and Law, C. S. 1993. Evidence for slow mixing across the pycnocline from an open-ocean tracer-release experiment. *Nature* **364**, 701–703.

Levitus, S. 1982. *Climatological atlas of the world ocean.* NOAA professional paper 13, 173 pp.

Madec, G. and Imbard, M. 1996. A global ocean mesh to overcome the North Pole singularity. *Climate Dyn.* **12**, 292–309.

Madec, G., Delecluse, P., Imbard, M. and Levy, C. 1998. *OPA Version 8.1, Ocean general circulation model reference manual.* Note du pôle de modélisation, IPSL, **11**, 91 pp.

Marsh, R., Nurser, A. J., Megann, A. P. and New, A. L. 2000. Water mass transformation in the Southern Ocean of a global isopycnal coordinate model. *J. Phys. Oceanogr*, in press.

Marshall, D. 1997. Subduction of water masses in an eddying ocean. *Jour. Mar. Res.* **55**, 201–222.

Sloyan, B. 1997. *The circulation of the Southern Ocean and the adjacent ocean basins determined by inverse methods.* PhD thesis, Institute of Antarctic and Southern Ocean Studies, University of Tasmania, Hobart, Australia, 310 pp.

Sloyan, B. and Rintoul, S. R. 2000. The Southern Ocean limb of the deep global overturning circulation. *J. Phys. Oceanogr*., in press.

Speer, K. G. 1997. A note on average cross-isopycnal mixing in the North Atlantic Ocean. *Deep-Sea Res.* **44**, 1981–1990.

Speer, K. G. and Tzipermann, E. 1992. Rates of water mass formation in the North Atlantic Ocean. *J. Phys. Oceanogr.* **22**, 93–104.

Tandon, A. and Garrett, C. 1996. On a recent parameterization of mesoscale eddies. *J. Phys. Oceanogr.* **26**, 406–411.

Terray, L., Sevault, E., Guilyardi, E. and Thual, O. 1996. *The OASIS 2.u User guide and reference manual.* CERFACS Tech. Rep. TR/CMGC/96-46, CERFACS, Toulouse, France.

Treguier, A.-M., Held, I. and Larichev, A. 1997. Parameterization of quasi-geostrophic eddies in primitive equation ocean models. *J. Phys. Oceanogr.* **27**, 567–580.

Visbeck, M., Marshall, J., Haine, T. and Spall, M. 1997. On the specification of eddy transfer coefficients in coarse-resolution ocean circulation models. *J. Phys. Oceanogr.* **27**, 381–402.

Walin, G. 1982. On the relation between sea-surface heat flow and thermal circulation in the ocean. *Tellus* **34**, 187–195.